Prediction and Experimental Verification of Bubble and Processing Characteristics in Blown-Film Extrusion

Khokan Kanti Majumder,[1] Yan Ding,[2] Graham Hobbs,[3] Sati N Bhattacharya[1]

[1]*Rheology and Materials Processing Centre, RMIT University, 124 Latrobe Street, Melbourne, Victoria 3000, Australia*
[2]*School of Mathematical and Geospatial Sciences, RMIT University, 124 Latrobe Street, Melbourne, Victoria 3000, Australia*
[3]*AMCOR Research and Technology, RMIT University, 124 Latrobe Street, Melbourne, Victoria 3000, Australia*

Received 8 December 2007; accepted 24 July 2008
DOI 10.1002/app.29219
Published online 2 December 2008 in Wiley InterScience (www.interscience.wiley.com).

ABSTRACT: Blown-film modeling is useful to the flexible packaging industry for predicting process and bubble characteristics, such as freeze line height (FLH), bubble diameter, and film thickness. The use of a suitable rheological equation to describe material properties is critical in simulating the blown-film process. In this article, we present an improved rheological constitutive equation, which incorporates more realistic parameters of stress and deformation properties of the materials by combining the Hookean model with the Phan-Thien Tanner (PTT) model. The proposed PTT–Hookean model is aimed at enhancing the viscoelastic behavior of the melt during biaxial stretching in the blown-film extrusion. Predictions of the blown-film bubble characteristics and FLH obtained with the PTT–Hookean model agreed well with the experimental data of this study and previous studies with different materials and different die geometries. The justification for combining the Hookean model with the PTT model in the blown-film process is also reported here. © 2008 Wiley Periodicals, Inc. J Appl Polym Sci 111: 2657–2668, 2009

Key words: crystallization; extrusion; modeling; rheology; simulations

INTRODUCTION

The blown-film process involves the biaxial stretching of annular extrudate to make a suitable bubble according to the requirements of a product. During this film-blowing process (see Fig. 1), molten polymer from the annular die is pulled upward by the take-up force; air is introduced at the bottom of the die to inflate the bubble, and an air ring is used to cool the extrudate. The nip rolls are used to provide the axial tension needed to pull and flatten the film into the winder. The speed of the nip rolls and the air pressure inside the bubble are adjusted to maintain the process and product requirements. At a certain height from the die exit, the molten polymer is solidified by the effect of cooling followed by crystallization. This height is called the freeze line height (FLH). After the FLH, the bubble diameter is assumed to be constant. Depending on the rheological properties of polymer and the cooling rate, the FLH and film properties vary with a nonlinear relation between them. This is the reason that majority of the modeling and simulations of the film-blowing process in the literature[1–6] have focused on the region between the die exit and the freeze line.

During the film-blowing process, the take-up force is balanced by the axial component of the forces arising because of the deformation of the melt and the circumferential force due to the pressure difference across the film. Generally, rheological constitutive equations combined with fundamental film-blowing equations[7,8] are solved to simulate the film-blowing process. The stress, deformation tensor, and rate of deformation tensor derived from the rheological constitutive equations are directly used in the film-blowing equations along with the key parameters of the material, such as the relaxation time, slippage parameter of the polymer chain, zero-shear viscosity, zero-shear modulus, and flow activation energy. Hence, the strength and suitability of the rheological constitutive equations have a great impact on the prediction of bubble and processing characteristics from the modeling.

During biaxial stretching, the polymer is a complex liquid near the die exit. It then gradually changes to a solidlike material as it moves toward the FLH because of heat transfer and crystallization. A liquidlike model can be used to predict the rheological properties of the polymer close to the die exit, and a solidlike model is more suitable for the material approaching the FLH. Therefore, much research has focused on the development of a rheological model to

Correspondence to: S. Bhattacharya (sati.bhattacharya@rmit.edu.au).

Contract grant sponsors: Australian Research Council (linkage research grant and postgraduate scholarship for K.K.M).

© 2008 Wiley Periodicals, Inc.

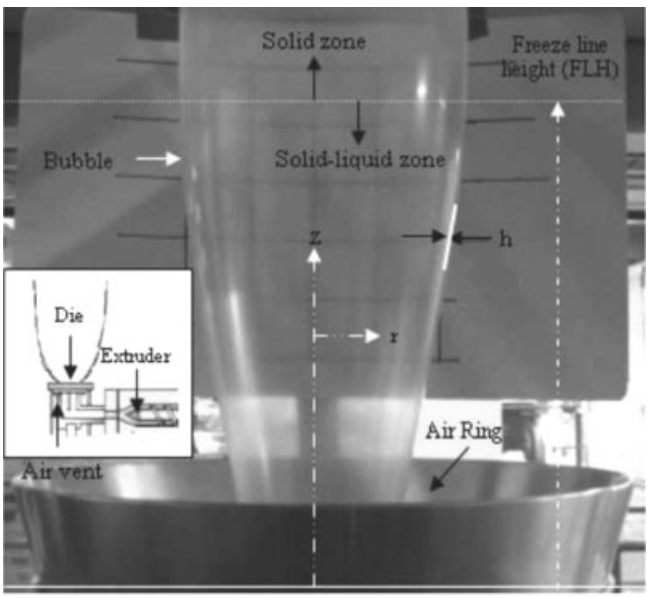

Figure 1 Blown-film production at the pilot plant.

satisfy the material's stress and deformation properties between the die exit and the FLH where a liquid-to-solid transition is involved.[2,3,5,9]

Following the blown-film modeling of Han and Park,[10] Khonakdar et al.[2] solved the modeling equations using assumed values of FLH, blow-up ratio, film thickness, and film temperature. The integration was carried out from the FLH to the die exit. They found that the film thickness value met closely with the die-exit data, whereas a variation of the blow-up ratio was observed at the die exit. The rate of deformation in the transverse direction might have been responsible for the variations in the bubble size. Muke et al.[3] developed a blown-film model using the Kelvin model to consider the viscoelastic effect of commercial polypropylene homopolymer (MA-3) and reported good agreement between their modeling results and the experimental data of bubble characteristics (e.g., diameter, thickness, temperature). However, their results did not show the stress relaxation behavior of the material, which is an important parameter in the film-blowing process, and it is well known that the prediction of the stress relaxation behavior is poor from the Kelvin model.[11]

For the nonisothermal study of the Maxwell model, Luo and Tanner[5] reported the bubble shapes of 14 nonisothermal runs [4 runs with a blow-up ratio (BUR) > 1 and 10 runs with BUR < 1]. For the 4 runs with BUR > 1, a reasonable agreement of the experimental data was obtained. However, no convergent results were obtained for BUR < 1 because of numerical instability. The transient behavior and stability of the film-blowing process were studied by Hyun et al.[9] with the viscoelastic Phan-Thien Tanner (PTT) model. Because of the consideration of the complex nonlinear nature of the partial differential equations and the boundary conditions, the dynamics of the blown-film process predicted from this study[9] were more realistic. Although film crystallinity is an important factor for blown-film process dynamics as reported by Pirkle and Braatz,[12] the crystallization kinetics of the melts were not considered in this modeling,[9] and the predictions were limited from the die exit to the FLH.

Blown-film modeling incorporating crystallization properties and viscoelasticity were reported by Muslet and Kamal[4] with the PTT and neo-Hookean models. Their simulation results showed good agreement with the experimental data obtained by Butler et al.[13] and Ghaneh-Fard et al.[14] Nevertheless, Muslet and Kamal's[4] results also showed that the film thickness continued to decrease after the FLH, at which point a stable bubble size had already been achieved at the FLH for material G [linear low-density polyethylene (LDPE)]. This indicated that their rheological equations might have predicted the results inadequately near the FLH. Several other studies of some specific aspects of blown-film modeling have also been reported in the literature.[1–5,9,10,15–18]

The majority of blown-film modeling[3,4,8] has started with assumed values of the FLH and bubble characteristics at the FLH, which were then traced back to match the die-exit parameters. However, the polymer film industry is more interested in the development of a mathematical model that can predict FLH and, consequently, realistic values of the bubble characteristics (diameter, thickness, and temperature) at the FLH, given the die-exit parameters. From a practical point of view, the industry also requires the model prediction to be efficient with acceptable accuracy. To meet industrial requirements, a modified rheological constitutive equation has been developed and is presented in this article. The significance of the modified rheological constitutive equation is to incorporate the most realistic values of the stress and deformation properties near the FLH in the blown-film model by the combination of the PTT model with the Hookean model; this is solved for a steady-state solution. The processing characteristics predicted with this model were verified with the pilot-plant data and the experimental data of Muke et al.[3] Justification for the use of the Hookean model (solidlike) with the PTT model (liquidlike) in the blown-film modeling is also presented here with identical processing conditions of two different LDPEs.

GOVERNING EQUATIONS OF THE FILM-BLOWING PROCESS

The governing equations presented here are based on the following assumptions: (1) all stresses in the

molten polymer develop before the die exit has been relaxed; (2) the flow of the molten polymer is homogeneous under biaxial extension;[4] (3) the process is in a steady state, and the bubble is axisymmetric[5] with respect to the vertical axis (z direction in Figs. 1 and 2); and (4) the die swell, inertia, gravity, surface tension, and air drag effects are neglected.[7,8]

Fundamental film-blowing equations

With regard to the thin-film bubble membrane studied by Pearson and Petrie,[7,8] the bubble was assumed to have two radii of curvature, R_1 (in the machine direction) and R_3 (in the transverse or hoop direction), which could be expressed in terms of the following expressions:

$$R_1 = \frac{-\sec^3\theta}{d^2r/dz^2} = \frac{-[1+(dr/dz)^2]^{3/2}}{d^2r/dz^2} \quad (1)$$

$$R_3 = \frac{r}{\cos\theta} = r\sqrt{1+(dr/dz)^2} \quad (2)$$

$$\tan\theta = \frac{dr}{dz} \quad (3)$$

where θ is the angle of film blowing and r is the dimensionless local bubble radius. According to the conservation of mass, the mass flow rate ($\dot{m}$) is calculated as

$$\dot{m} = \pi(r_0^2 - r_i^2)v_0\rho_m = 2\pi\rho_s rHV \quad (4)$$

where r_0 and r_i are the outer and inner radii of the die opening; v_0 and V are the linear velocities of the bubble at the die opening and at the freeze line, respectively; ρ_m and ρ_s are the densities of the material in the molten and solid states, respectively; and H is the local film thickness. Therefore, for incompressible materials, the volumetric flow rate (Q) through the die is as follows:

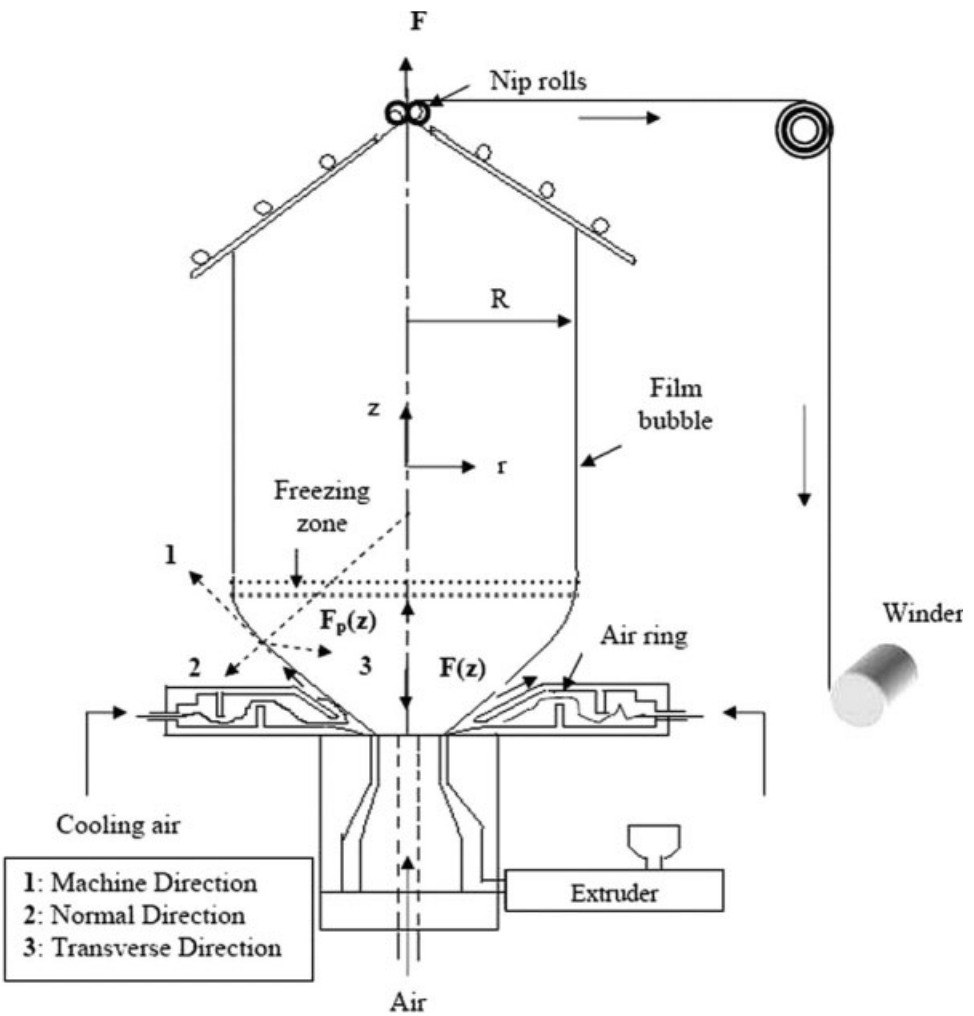

Figure 2 Schematic diagram of the blown-film process with surface coordinates and free-body diagram of the forces.

$$Q = 2\pi r H v_{\mathrm{m}} = \text{Constant} \tag{5}$$

where v_m is the velocity in the meridional (machine) direction. The velocity in the transverse direction is zero because of the axisymmetric nature of the bubble. The velocity in the thickness or normal direction is not exactly zero but negligible because the film is of changing the thickness from the die exit to FLH.[5]

The derivative of eq. (5) with respect to z (the distance along the film blowing) yields a relation between the deformation rates in the blowing:[3]

$$\frac{dv_m}{dz} = -\frac{1}{H} v_m \frac{dH}{dz} - \frac{1}{r} v_m \frac{dr}{dz} \tag{6}$$

where $\frac{dv_m}{dz}$, $-\frac{1}{H} v_m \frac{dH}{dz}$, and $-\frac{1}{r} v_m \frac{dr}{dz}$ represent the rates of stretching along the machine, normal, and transverse directions, respectively.

If one considers that a small amount of material is in equilibrium under a set of membrane forces, the equilibrium equation of the stresses in the normal (thickness) direction is as follows:[5]

$$\frac{\Delta P}{H} = \frac{\sigma_m}{R_1} + \frac{\sigma_t}{R_3} \tag{7}$$

where ΔP is pressure variation, or the internal pressure measured relative to the atmospheric pressure, and σ_m and σ_t are the principal stresses in the machine and transverse directions, respectively.

Replacing R_1 and R_3 in eq. (7) yields

$$\frac{\Delta P}{H} = \cos\theta \left(\frac{\sigma_t}{r} - \sigma_m \frac{d\theta}{dz} \right) \tag{8}$$

According to previous studies,[3,6] the total force (F) is balanced by $F(z)$, $Fg(z)$, and $Fp(z)$ in Figure 2, as shown in the following equation:

$$F = F(z) + Fg(z) - Fp(z) \tag{9}$$

where $F(z)$ is the axial component of the force generated because of the deformation of the material, $Fp(z)$ is the force due to the pressure difference between the inside and outside of the bubble, and $Fg(z)$ is the force due to gravity. In this study, $Fg(z)$ was neglected. Hence

$$F(z) = Fp(z) + F \tag{10}$$

$$F(z) = -\Delta P \pi (r^2 - r_0^2) + 2\pi H r \sigma_m \cos\theta \tag{11}$$

where

$$\cos\theta = \left[1 + \left(\frac{dr}{dz} \right)^2 \right]^{-1/2} = \frac{1}{\sqrt{1 + r'^2}}$$

Differentiating eq. (11) and arranging it with eq. (8) yields

$$\sigma'_m = \sigma_m \left(\frac{r'}{r} \left(\frac{\sigma_t}{\sigma_m} - 1 \right) - \frac{H'}{H} \right) \tag{12}$$

In the previous equations and hereafter, the prime ($'$) refers to the derivatives with respect to the dimensionless distance from the die exit in the axial direction z.

Rearranging and combining eqs. (1)–(12) gives the dimensionless fundamental film-blowing equations regardless of the rheological constitutive equations:[3]

$$L = \frac{(A + Br^2)\sqrt{1 + r'^2}}{rh} \tag{13}$$

$$r'' = \frac{[hC\sqrt{1 + r'^2} - 2rB(1 + r'^2)]}{A + Br^2} \tag{14}$$

where L is the dimensionless stress in the machine direction:

$$L = \frac{r_0 \sigma_{11}}{\eta_0 v_0}$$

where σ_{ij} is the principal stress on the bubble, η_0 is the zero-shear viscosity. A is the dimensionless tensile force:

$$A = \frac{F_z r_0}{\eta_0 Q} - B \left(\frac{r_f}{r_0} \right)^2$$

where r_f is the bubble radius at the freeze line height (FLH), F_z is the tensile force at the freeze line. B is the dimensionless bubble pressure:

$$B = \frac{\pi r_0^3 \Delta P}{\eta_0 Q}$$

h is the dimensionless film thickness, r'' is the second-order derivative of the dimensionless bubble radius with respect to the dimensionless distance in the axial direction z, and C is the dimensionless stress in the transverse direction:

$$C = \frac{r_0 \sigma_{33}}{\eta_0 v_0}$$

Rheological constitutive equations

The rate of the deformation tensor ($\dot{\varepsilon}$) in the surface coordinate system can be expressed in terms of the dimensionless film velocity (v), bubble radius, film thickness, angle of film blowing, and the distance from the die:

$$\dot{\varepsilon}_{ij} = v \cos\theta \begin{pmatrix} \frac{1}{v}\frac{dv}{dz} & 0 & 0 \\ 0 & \frac{1}{h}\frac{dh}{dz} & 0 \\ 0 & 0 & \frac{1}{r}\frac{dr}{dz} \end{pmatrix} \tag{15}$$

In this study, total stress (τ_i) is proposed to be the combination of the stresses in the molten state (τ_m) and the solid state (τ_s):

$$\tau_i = \tau_m + \tau_s \tag{16}$$

where τ_m is calculated with the PTT model and τ_s is calculated with the Hookean model.

According to the previous studies,[4,9] the PTT model for the molten state is expressed as follows

$$2\eta\dot{\varepsilon}_i = \tau_i Y(\tau) + \lambda\left[\overset{\nabla}{\tau}_i + 2\xi(\tau_i\dot{\varepsilon}_i)\right] \tag{17}$$

These symbols are related to eq. (17) as referred from the literature.[4,9] In eq. (17), η is the viscosity, Y is the dimensionless function for extensional flow properties and $\overset{\nabla}{\tau}_i$ is the upper convective time derivatives for expressing deformation rate history.[4,9] Where $\dot{\varepsilon}_i$ is the deformation rate tensor, τ is the deviatoric stress, λ is the relaxation time, and ξ is the slippage parameter of the polymer chains in the PTT model.[4] So, the total stress can be calculated as

$$\tau_i = \tau_i Y(\tau) + \lambda[\overset{\nabla}{\tau}_i + 2\xi(\tau_i\dot{\varepsilon}_i)] + 2G_0\varepsilon_i \tag{18}$$

where G_0 is the zero-shear elastic modulus and

$$\overset{\nabla}{\tau}_i = \frac{d\tau}{dt} - [\nabla v][\tau_i] - [\tau_i][\nabla v]^t$$

$$Y(\tau) = \exp\left(\frac{\varepsilon\lambda}{\eta} tr\tau_i\right)$$

where ε is the extensional property of the film in the PTT model.[4]

The strain and rate of strain acting on an element of fluid in each of the principal directions are given as[3]

$$\varepsilon_{11} = \ln\left(\frac{v}{v_0}\right) = \ln\left(\frac{r_0H_0}{rH}\right) \tag{19a}$$

where the subscript 0 refers to conditions at the die exit (e.g., H_0 is the local film thickness at the die exit).

$$\varepsilon_{22} = \ln\left(\frac{H}{H_0}\right) \tag{19b}$$

$$\varepsilon_{33} = \ln\left(\frac{r}{r_0}\right) \tag{19c}$$

$$\dot{\varepsilon}_{11} = \frac{v}{\sqrt{1+r'^2}}\left(-\frac{H'}{H} - \frac{r'}{r}\right) \tag{19d}$$

$$\dot{\varepsilon}_{22} = \frac{vH'}{H\sqrt{1+r'^2}} \tag{19e}$$

$$\dot{\varepsilon}_{33} = \frac{vr'}{r\sqrt{r+r'^2}} \tag{19f}$$

Hence, the deviatoric stresses (τ_{ij}'s) in each of the principal directions are

$$\frac{d\tau_{11}}{dz} = \frac{1}{\lambda v\cos\theta}\left(\tau_{11}(1 - Y(\tau) + 2(1-\xi)\lambda\dot{\varepsilon}_{11}) - 2G_0\varepsilon_{11}\right) \tag{20a}$$

$$\frac{d\tau_{22}}{dz} = \frac{1}{\lambda v\cos\theta}\left(\tau_{22}(1 - Y(\tau) + 2(1-\xi)\lambda\dot{\varepsilon}_{22}) - 2G_0\varepsilon_{22}\right) \tag{20b}$$

$$\frac{d\tau_{33}}{dz} = \frac{1}{\lambda v\cos\theta}\left(\tau_{33}(1 - Y(\tau) + 2(1-\xi)\lambda\dot{\varepsilon}_{33}) - 2G_0\varepsilon_{33}\right) \tag{20c}$$

The total stress for each of the components is related to the deviatoric stresses of the constitutive equations[3] by

$$\sigma_{ij} = \tau_{ij} - p\delta_{ij} \tag{21}$$

where p is the isotropic pressure and δ_{ij} is the Kronecker delta: $\delta_{ij} = \begin{Bmatrix} 1 & i=j \\ 0 & i\neq j \end{Bmatrix}$. The stress at the free surface is equal to atmospheric pressure.[3] This gives

$$p = \tau_{22}$$

Hence

$$\sigma_{11} = \tau_{11} - \tau_{22} \tag{22}$$

and

$$\sigma_{33} = \tau_{33} - \tau_{22} \tag{23}$$

Introducing the following dimensionless terms into the previous equations [eqs. (21)–(23)]

$$h = \frac{H}{H_0}$$

$$r = \frac{R}{r_0}$$

$$z = \frac{Z}{r_0}$$

$$v = \frac{V}{v_0}$$

$$t = \frac{T - T_a}{T_a}$$

(where t is the dimensionless temperature, T is the temperature, and T_a is the ambient air temperature)

$$De = \frac{\lambda v_0}{r_0} = \frac{\eta_0 v_0}{G_0 r_0}$$

(where De is the Deborah number)

$$\eta = \frac{\eta(T)}{\eta_0}$$

$$L = \frac{r_0\sigma_{11}}{v_0\eta_0}$$

$$C = \frac{r_0\sigma_{33}}{v_0\eta_0}$$

and rearranging these equations gives the differential stresses with respect to z in the machine, transverse, and normal (thickness) directions, respectively:

$$L' = \frac{L}{De}[1 - Y(\tau)] - 2(1-\xi)\left[\frac{Lv}{\sqrt{1+r'^2}}\left(\frac{h'}{h} + \frac{r'}{r}\right)\right] - 2(1-\xi)\left[\frac{Pv}{\sqrt{1+r'^2}}\left(\frac{2h'}{h} + \frac{r'}{r}\right)\right] - \frac{2\ln(1/rh^2)}{De^2} \quad (24)$$

P is the dimensionless stress in normal direction.

$$C' = \frac{C}{De}[1 - Y(\tau)] + 2(1-\xi)\left[\frac{r'Cv}{r\sqrt{1+r'^2}}\right] + 2(1-\xi)\left[\frac{Pv}{\sqrt{1+r'^2}}\left(\frac{h'}{h} + \frac{r'}{r}\right)\right] - \frac{2\ln(r/h)}{De^2} \quad (25)$$

$$\tau'_{22} = \frac{P}{De}(1 - Y(\tau)) - \frac{2\ln(h)}{De^2} + \frac{2(1-\xi)Pvh'}{h\sqrt{1+r'^2}} \quad (26)$$

where

$$Y(\tau) = \exp\left(\frac{\varepsilon De}{\eta}(\tau_{11} + \tau_{22} + \tau_{33})\right)$$

Equations (13), (14), and (24)–(26) are combined to obtain the following nonlinear differential equation to determine the bubble characteristics:

$$\frac{h'}{h}\left[1 - 2(1-\xi)\frac{v}{\sqrt{1+r'^2}}\left(1 + \frac{2P}{\sigma_{11}}\right)\right] = \frac{r'}{r}\left(\frac{\sigma_{33}}{\sigma_{11}} - 1\right) - \frac{1}{De}(1 - Y(\tau)) + \frac{2(1-\xi)r'v}{r\sqrt{1+r'^2}}\left(1 + \frac{P}{\sigma_{11}}\right) + \frac{2}{De^2}\ln\left(\frac{1}{rh^2}\right) \quad (27)$$

Although complex thermodynamics are involved during the film-blowing process because of the effect of cooling air and other process dynamics, most blown-film modeling[1,3,5,15] has ignored the effect by the treatment of the heat-transfer coefficient as a constant. In this study, the thermodynamic effect is considered by the incorporation of a modified heat-transfer function [eq. (28)] from previous studies[4,19] with the dimensionless energy equation.[5] The end effect of the cooling air at the lip of the die exit and after the FLH was not considered in eq. (28). Equation (28) incorporates the effects of the temperature difference between the film surfaces, the velocity of the cooling air, and the radius of the bubble on the heat-transfer coefficient (H_c):

$$H_c = \frac{0.084V_{\text{air}}\lfloor 560 - 780\exp(-1.27(T_{\text{surface}} - T_{\text{air}}) - 0.035r)\rfloor}{1 + \exp(z)} \quad (28)$$

Consequently, the dimensionless energy equation[5] used in this study is

$$t' = C_e\left[C\frac{r'}{r} - L\left(\frac{h'}{h} + \frac{r'}{r}\right)\right] - C_h rt\sqrt{1+r'^2} \quad (29)$$

where $C_e = \eta_0 Q/2\pi a_0^2 h_0 \rho C_p T_a$ (a_0 is the bubble radius at the die exit) is the dimensionless energy dissipation coefficient and $C_h = 2\pi a_0^2 H_c/\rho C_p Q$ is the dimensionless heat-transfer coefficient, where ρ is the density and C_p is the specific heat of the polymer.

According to previous studies,[3,5] the following temperature dependence of the viscosity function (Arrhenius type) is used here:

$$\eta_0(T) = \eta_0(T_0)\exp\left[E_a\left(\frac{1}{T} - \frac{1}{T_0}\right)\right] \quad (30)$$

where $\eta_0(T)$ is the zero-shear viscosity as a function of temperature, $\eta_0(T_0)$ is the zero-shear viscosity at the die exit, T_0 is the die temperature, and E_a is the flow activation energy of the polymer.

In summary, the newly established viscoelastic model uses the PTT model (a well-known nonlinear viscoelastic rheological model describing the melt-flow behavior (Hyun et al.[9]) instead of the Newtonian model (as used in the Kelvin model) together with the Hookean model. Thus, the PTT–Hookean model has the capability of predicting nonlinear behavior of the melt at high deformations.

NUMERICAL TECHNIQUES AND INITIAL AND BOUNDARY CONDITIONS

A fourth-order Runge–Kutta method (Kutta–Simpson 1/3 rule) is used to solve the set of steady-state film-blowing equations presented in the previous section [eqs. (13), (14), (24)–(27), and (29)] simultaneously. To ensure the stability of the solution, a step size of 0.01 is used. The codes were written in Maple Version 10 for the numerical integration. The solving process initiates from the die exit with the input parameters as shown later in Table II and continues until the changes in the bubble expansion and thickness reduction with respect to the dimensionless axial distance become negligible or approach zero ($\frac{dr}{dz} \approx 0$ and $\frac{dh}{dz} \approx 0$). The solving process is terminated once these are achieved. The axial distance from the die exit to the location of termination is then considered to be the predicted FLH.

TABLE I
Molecular Characteristics of the LDPEs Obtained from the Gel Permeation Chromatography Study

Resin property	LDPE-1 (Pol-1)	LDPE-2 (Pol-2)
Weight-average molecular weight (M_w)	167,000	135,000
Number-average molecular weight (M_n)	17,600	15,500
Z-average molecular weight	610,000	515,000
Molecular weight distribution (M_w/M_n)	9.48	8.71
Branching index	0.24	0.32
Branches per Dalton	1.45×10^{-3}	8.40×10^{-4}
Branches per 1000C	20	12

The boundary conditions at the die exit ($z = 0$) are $r = 1$ (bubble diameter is equal to the die diameter), $h = 1$ (bubble thickness is equal to the die gap), and $t = \frac{T_{\text{die}} - T_a}{T_a}$, where T_{die} is the temperature at the die exit.

EXPERIMENTAL DATA

Shear rheology

Compression-molded samples of the LDPEs [Pol-1 and Pol-2 (Table I)] 2 mm thick prepared at 200°C and a force of 120 kN were cut into discs 25 mm in diameter for the shear rheological test. Dynamic and steady-shear rheological properties were obtained with the Advanced Rheometrics Expansion System rheometer (ARES). All measurements in the ARES were performed with a force transducer in a torque range between 0.2 and 400 g cm. Steady-shear rheological data at higher shear rates (1–50 s^{-1}) were obtained from a Davenport capillary rheometer. Rheological measurements of MA-3 were described elsewhere.[3]

The flow activation energies were calculated with eq. (31) as 57.03 and 52.01 kJ/mol for Pol-1 and Pol-2, respectively, which provided a good indication of the higher degree of long-chain branching for Pol-1.[20] A modified Cross model [eq. (32)] was used to measure the zero-shear viscosity with the ARES and the capillary rheometer data of the resins. Discrete relaxation spectrum data from the ARES was used to calculate the average relaxation time (λ_{Avg}) with eq. (33):

$$a_{\text{T}} = \exp\left[\frac{E_a}{R}\left(\frac{1}{T} - \frac{1}{T_0}\right)\right] \tag{31}$$

where a_T is the shift factor and R is the universal gas constant:

$$\eta(T) = \frac{\eta_0(T)}{1 + K_2\dot{\gamma}^m} \tag{32}$$

where $\dot{\gamma}$ is the shear rate and K_2 and m are model constants:

$$\lambda_{Avg} = \frac{\sum G_k\lambda_k^2}{\sum G_k\lambda_k} \tag{33}$$

TABLE II
Rheological and Processing Parameters of the Resins Used in the Modeling

Input	Pol-1	Pol-2	MA-3[3]
ρ (kg/m^3)	922	922	900
η_0 (Pa s)	96,503 (at 200°C)	26,000 (at 200°C)	22,800 (at 210°C)
λ (s)	14.65 (at 200°C)	1.74 (at 200°C)	18.4 (at 210°C
E_a/R (K)	6860	6255	4924
$\dot{m}$ (kg/h)	7.5	7.5	3.9
T_a (°C)	25	25	25
T_{die} (°C)	200	200	210
Die diameter (mm)	65	65	40
H_0 (mm)	2.038	2.038	0.75
Crystallization temperature (°C)	103	102	123
De_0 ($\lambda v_0/r_0$)	5.86	0.696	7.11
ε[4]	0.05	0.05	0.05
ξ[4]	0.147	0.147	0.147
v_0 (m/s)	0.013	0.013	0.0077
A	0.61	0.61	0.83885
B	0.2035	0.2035	0.38773
C_e	0.000034402	0.00000932	0.00002234

where G_k is the relaxation modulus and λ_k is the relaxation time.

Pilot-plant study

An advanced extrusion blown-film coextrusion assembly (diameter = 20 mm, length/diameter = 30 : 1 and compression ratio = 2.2 : 1 for Screw-1 and Screw-3 and diameter = 25 mm, length/diameter = 30 : 1, and compression ratio = 2.8 : 1 for Screw-2) manufactured by Future Design, Inc., was used to process the LDPE resins at AMCOR Research and Technology's blown-film pilot plant (Mississauga, Ontario, Canada). A die geometry with a 2.032-mm gap and 65-mm diameter was used in this study. Films were produced at 200°C (die temperature) and four different blower settings (2.4, 2.6, 2.8, and 3.0, which corresponded to average air velocities of 6.7, 7.2, 7.7, and 8.2 m/s, respectively outside of the bubble). The speed of the screws was kept constant to maintain an average mass flow rate of 7.5 kg/h. The nip roller speed was equipped with a sophisticated controlled device of digital output. With a digital micrometer, the final film thickness of Pol-1was measured at about 110–120 μm (μm).

RESULTS AND DISCUSSION

The prediction of the FLH and bubble characteristics (diameter, thickness, and temperature) at the FLH were the main objectives of this study. Therefore, it is necessary to discuss the modeling outputs first, that is, whether they showed a realistic prediction, before they are compared with the experimental data. According to previous studies,[4,9] the PTT model is the best to describe the stress and deformation properties of a polymer when it is in the molten state and in the field of extension. Therefore, the prediction may not be correct close to the freezing line if only the PTT model is used. A solidlike rheological model, such as the Hookean model, may make better predictions close to the FLH because the phase of the material is almost in a solid state when it is close to the freezing line. Furthermore, a significant region between the die exit and the FLH deals with a liquid–solid phase transition because of heat transfer arising from the cooling effect. This is a highly nonequilibrium complex dynamic process.

There has been no a widely accepted rheological model presented in the literature to describe the stress and deformation properties during this liquid–solid phase transition. The current PTT model could fit both liquid and solid behavior of the polymer melt if proper functional expressions and equations were used in the governing equations of the blown-film system. The dynamic solution of such a system in obtaining the FLH as the moving boundary of the partial differential equations in the governing equations could be very time-consuming and expensive, particularly when one is dealing with the stability and multiplicity issues of the solutions. This is, indeed, the main objective of the future research of this project. However, at this stage, to satisfy the demand of the industry, a practical rheological constitutive equation is proposed [see eq. (16)]. This model simply combines the PTT and the Hookean model to describe the stress and deformation properties in the liquid–solid transition zone.

Considering the film crystallinity in the solid state, Muslet and Kamal[4] proposed a similar model that combined the PTT model and the neo-Hookean model for viscoelasticity of the material. However, their model predictions showed significant deformation of the film in all (machine, transverse, and thickness) directions after the FLH. This is impractical in the blown-film process and also contradictory to their results of the bubble diameter, which was predicted as constant after the FLH. In their work, a sharp transition was also observed in the predicted curve of the film thickness when the model input parameters were shifted from the liquid phase to the solid phase. Those issues were solved in this study by use of the proposed constitutive equation [eq. (18)] in the fundamental blown-film equations [eqs. (13) and (14)].

Verification of the modeling results

Instead of focusing on the blowing angle near the die, as was done in several studies,[4,5,15] or on any calculations after the FLH,[4,15] in this study, we focused on the prediction of the processing and bubble characteristics close to the FLH. The results of the bubble diameter predicted by this model are presented in Figure 3. Similar to earlier studies by Muslet and Kamal[4] and Luo and Tanner,[5] Figure 3 shows that the bubble diameter decreased as the Deborah number at the die exit ($De_0 = \lambda v_0/r_0$) increased for both materials (Pol-1 and Pol-2).

A realistic value of the heat-transfer coefficient is required to simulate an actual film process because of its rapid changes in temperature from the die exit to the FLH and above. Several studies[5,15,21] in the past have simulated the blown-film process with a constant value of the heat-transfer coefficient. In reality, the heat-transfer value is high at the die exit and then decreases along the direction of flow. In this study, a heat-transfer function [eq. (28)] was used with the energy equation [eq. (29)] to incorporate a better estimate of the heat-transfer coefficient (Fig. 4) to simulate the blown-film bubble characteristics from the die exit to the FLH. The results are given in Figure 5.

The rheological and processing parameters listed in Table II were used in the simulation of the blown-film process. Figure 5 presents the experimental and predicted values of the bubble diameter,

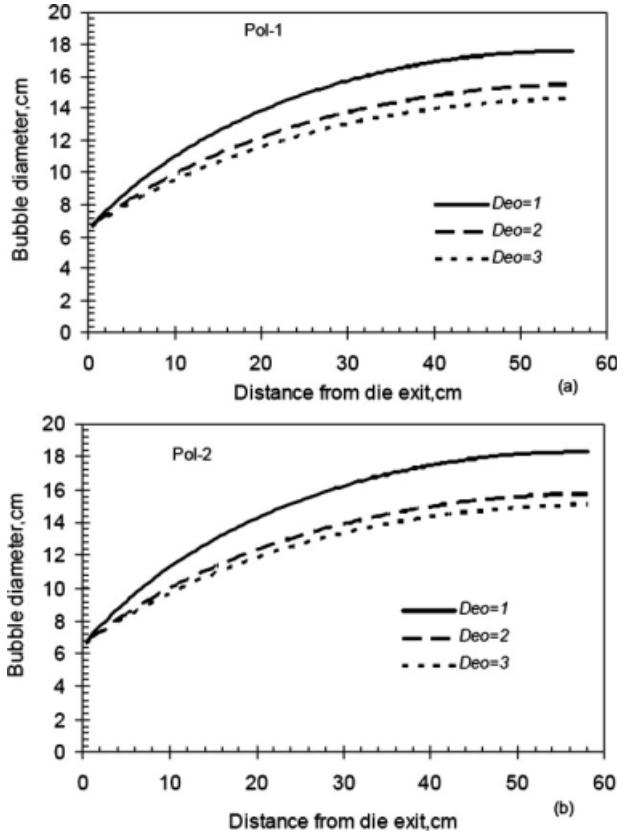

Figure 3 Effect of De_0 ($Deo = De_0 = \frac{\lambda v_0}{r_0}$) on the bubble shapes of (a) Pol-1 and (b) Pol-2.

thickness, and temperature of the film for two different materials (Pol-1 and MA-3) with different die geometries. The experimental data of MA-3 were obtained by Muke et al.[3] of the Rheology and Materials Processing Centre, RMIT University. We obtained the experimental data for Pol-1 using the pilot plant of the AMCOR Research and Technology, Melbourne. As shown in Figure 5, the experimental data for bubble diameter, film thickness, and film temperature of both polymers agreed reasonably well with the model predictions near the FLH. Also,

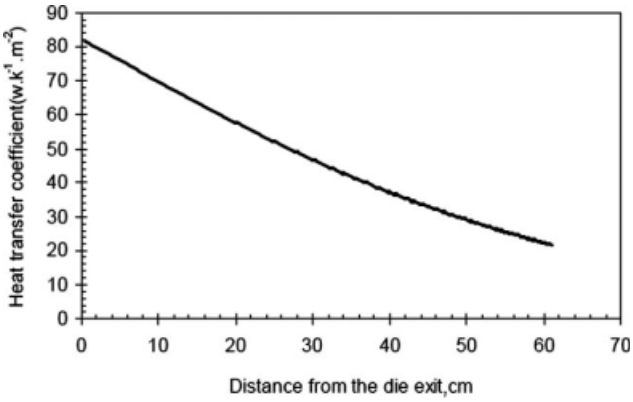

Figure 4 Prediction of the heat-transfer coefficient of Pol-1 with eq. (28).

there was no sharp transition in the thickness profile or any other deformations after the FLH, which was similar to an earlier study,[4] for both LDPEs. The model predictions of the bubble characteristics (diameter, thickness, and temperature) were smooth from the die exit to the FLH. These simulation results show that the proper values of the rheological properties were incorporated with the fundamental film-blowing equations. Because of the FLH instability[18] during processing, a variation in the FLH was observed between the experimental and predicted data (Fig. 5). The results from this study should be very practical and useful to the plastics

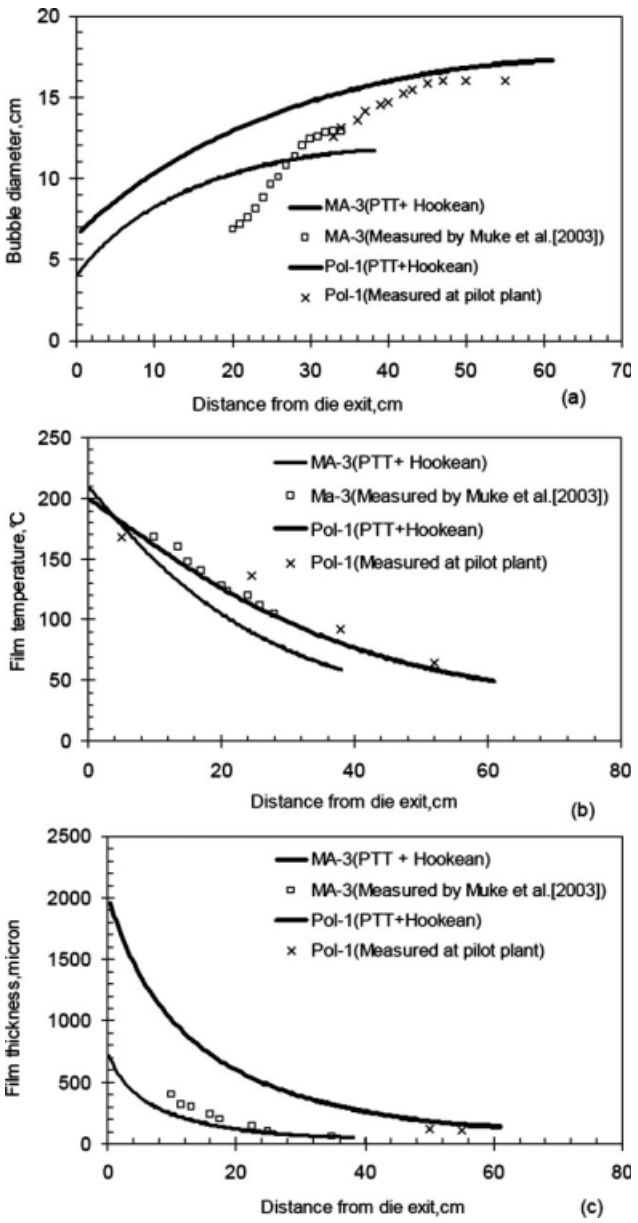

Figure 5 Verification of the modeling outputs with the experimental data obtained from a previous study[3] and this study: (a) bubble diameter, (b) film temperature, and (c) film thickness.

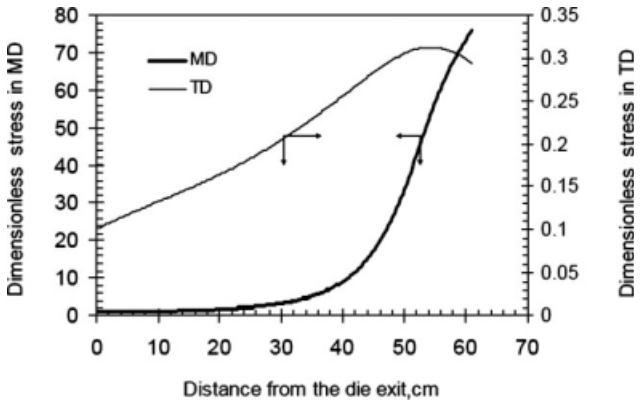

Figure 6 PTT–Hookean model prediction of the stresses in the machine direction (MD) and transverse direction (TD) for Pol-1.

industry for the selection of suitable materials for customized and large-scale productions.

Stress and strain rate predicted from the PTT–Hookean model are presented in Figures 6 and 7. Higher values of strain rate and stresses were found in the machine direction than in the transverse direction. These values showed realistic predictions in both directions, although the experimental data for stress and strain rate are not available here. Figure 6 shows that the stress in the transverse direction increased from the die exit and then dropped near the FLH. The strain rate in the transverse direction was predicted to be higher near the die exit (Fig. 7) and then decreased to the lower values near the FLH. The prediction of the strain rate in the machine direction (Fig. 7) increased from the die exit and then dropped near the FLH. These data show that the PTT–Hookean model was able to describe the stress and deformation properties of the polymer in a realistic way. Therefore, the simulated results of the bubble diameter, film thickness, and film temperature of the polymers (Pol-1 and MA-3) with the PTT–Hookean model conformed to the experimental data (Fig. 5).

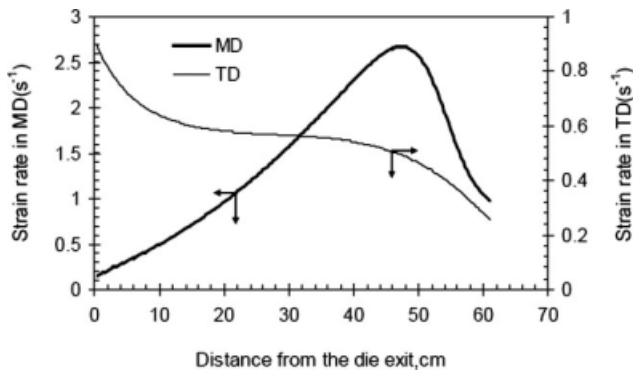

Figure 7 PTT–Hookean model predictions of the strain rate in the machine direction (MD) and transverse direction (TD) for Pol-1.

Significance of the PTT–Hookean model in numerical simulations

As discussed in previous sections, the PTT model gives accurate predictions for materials with certain

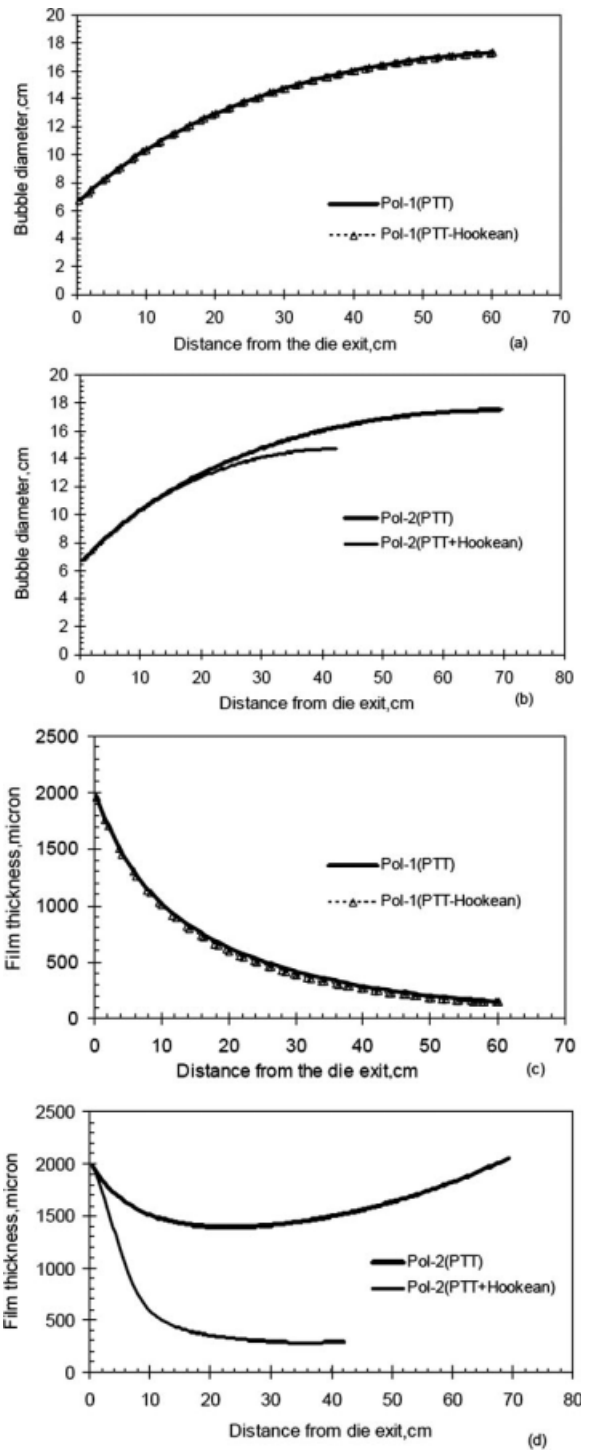

Figure 8 Comparisons of the numerical stabilities in the predictions of the PTT model and PTT–Hookean model for the LDPEs with a higher value of De_0 (Pol-1) and a lower value of De_0 (Pol-2), respectively: (a) bubble diameter for Pol-1, (b) bubble diameter for Pol-2, (c) film thickness for Pol-1, and (d) film thickness for Pol-2.

properties. This was also confirmed by the transient study of the blown-film modeling with the PTT model by Hyun et al.[9] They found good agreement between their predicted and experimental results. In this study, the predictions for Pol-1 from both the PTT and PTT–Hookean models agreed very well, as shown in Figure 8(a,c). However, the PTT and PTT–Hookean models gave different predictions for Pol-2, as shown in Figure 8(b,d). Figure 8(b) shows an extra FLH and an increased bubble diameter for Pol-2 as predicted with the PTT model as compared to the predictions with the PTT–Hookean model. Furthermore, the thickness prediction of Pol-2 from the PTT model showed that the thickness of the film continued to increase at and after the FLH [see Fig. 8(d)]. This was not realistic, as the thickness of the film should have been constant when it reached the FLH, as predicted from the PTT–Hookean model [see Fig. 8(d)].

The relaxation time and melt elasticity of the material might have been the controlling factors in the calculation of the deformation near the die exit, which gave incorrect predictions for Pol-2 with the PTT model. Luo and Tanner[5] reported that De_0 is a solidlike or elastic parameter, which controls the stretching. The larger value of De_0 represents the more solid like response of the material. For Pol-1, De_0 was 5.86, whereas it was 0.696 for Pol-2. Because of the higher melt elasticity and relaxation time (Table II) of Pol-1, the predictions from the PTT–Hookean model were nearly identical to the predictions from the PTT model [see Fig. 8(a,c)]. For Pol-2, with a low De_0 value, the predictions from the PTT–Hookean model were much more realistic than those from the PTT model, as shown in Figures 8(b,d). To further investigate the effect of De_0 on the PTT model, a series of film thickness predictions with the PTT model with various values of De_0 were carried out. The results are presented in Figure 9. As shown in Figure 9, the effect of De_0 on the prediction of film thickness with the PTT model was significant, as realistic predictions were observed only at higher De_0 values with the PTT model. Figure 9 also presents the prediction of film thickness with the PTT–Hookean model for the material (Pol-2) with lower melt elasticity ($De_0 = 0.7$). The prediction was much more realistic than that obtained from the PTT model. Therefore, we concluded that the PTT–Hookean model was more suitable for describing the real processing and bubble characteristics when materials with lower values of melt elasticity and relaxation time are used in a blown-film simulation.

Transient simulations would provide more accurate solutions for dynamic processes such as blown-film extrusion. However, a steady-state simulation is more practical, as it has the advantages of being simple, efficient, and able to provide the predictions accurate enough to meet the needs of the industry.

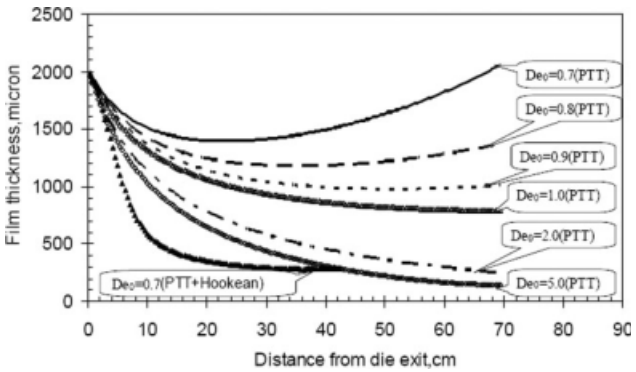

Figure 9 Effect of De_0 ($De_0 = De_0$) of Pol-2 in the prediction of the blown-film thickness with the PTT model and the model of this study.

CONCLUSIONS

In this article, the necessity of a suitable rheological equation was justified for obtaining improved predictions from blown-film modeling. The best possible values of the rheological properties were obtained with a combined PTT and Hookean model (PTT–Hookean), particularly for materials with lower melt elasticity and relaxation time. The PTT–Hookean model can

- Predict a realistic profile of bubble characteristics (diameter, thickness, and temperature).
- Predict the FLH with the die-exit data.
- Provide good agreement between the predicted values and the experimental results of this study and previous[3] studies.

NOMENCLATURE

A	Dimensionless tensile force
ARES	Advanced Rheometrics Expansion System rheometer
a_T	Shift factor
B	Dimensionless bubble pressure
BUR	Blow up ratio
C	Dimensionless stress in the transverse direction
C_e	Dimensionless energy dissipation coefficient
C_h	Dimensionless heat-transfer coefficient
C_p	Specific heat of the polymer
De	Deborah number
De_0	Deborah number at the die exit
E_a	Flow activation energy
F	Total force
FLH	Freeze line height
F_z	Tensile force at the freeze line
$F(z)$	Axial component of the force generated because of the deformation of the material
$Fg(z)$	Force due to gravity

$Fp(z)$	Force due to the pressure difference between the inside and outside of the bubble
G_0	Zero-shear elastic modulus
G_k	Relaxation modulus
h	Dimensionless film thickness
H	Local film thickness
H_c	Heat-transfer coefficient
K_2	Model constant
L	Dimensionless stress in the machine direction
LDPE	Low-density polyethylene
m	Model constant
$\dot{m}$	Mass flow rate
MA-3	Polypropylene homopolymer
M_n	Number-average molecular weight
M_w	Weight-average molecular weight
p	Isotropic pressure
ΔP	Pressure variation, or the internal pressure measured relative to the atmospheric pressure
PTT	Phan-Thien Tanner
Q	Volumetric flow rate
r	Dimensionless local bubble radius
R	Universal gas constant
r_0	Outer radius of the die opening
R_1	Radius of curvature in the machine direction
R_3	Radius of curvature in the transverse direction
r''	Second-order derivative of the dimensionless bubble radius with respect to the dimensionless distance in the axial direction z
r_i	Inner radius of the die opening
t	Dimensionless temperature
T	Temperature
T_0	Die temperature
T_a	Ambient air temperature
T_{die}	Temperature at the die exit
v	Dimensionless film velocity
V	Linear velocity at the freeze line
v_0	Linear velocity of the bubble at the die opening
v_m	Velocity in the machine direction
z	Dimensionless distance in the axial direction

Greeks

δ_{ij}	Kronecker delta
ε	Extensional property of the film in the PTT model
ε_i, ε_{ij}	Deformation tensor
$\dot{\varepsilon}_{ij}$	Deformation rate tensor
$\dot{\gamma}$	Shear rate
λ, λ_k	Relaxation time
λ_{Avg}	Average relaxation time
η_0	Zero-shear viscosity
$\eta_0(T)$	Zero-shear viscosity as a function of temperature
$\eta_0(T_0)$	Zero-shear viscosity at the die exit
ρ	Density
ρ_m	Density of the material in the molten state
ρ_s	Density of the material in the solid state
σ_m	Principal stress on the bubble in the machine direction
σ_t	Principal stress on the bubble in the transverse direction
θ	Angle of film blowing
τ, τ_{ij}	Deviatoric stress
τ_i	Total stress
τ_m	Stress in the molten state
τ_s	Stress in the solid state
ξ	Slippage parameter in the PTT model

Subscripts

0	Refers to conditions at the die exit
1 or m	Refers to conditions in the machine direction
2 or n	Refers to conditions in the normal or thickness direction
3 or t	Refers to conditions in the transverse or hoop direction

References

1. Kanai, T.; White, J. L. J Polym Eng Sci 1984, 24, 1185.
2. Khonakdar, H. A.; Morshedian, J.; Nodehi, A. O. J Appl Polym Sci 2002, 86, 2115.
3. Muke, S.; Connel, H.; Sbarski, I.; Bhattacharya, S. N. J Non-Newtonian Fluid Mech 2003, 116, 113.
4. Muslet, I. A.; Kamal, M. R. J Rheol 2004, 48, 525.
5. Luo, X.-L; Tanner, R. I. J Polym Eng Sci 1985, 25, 620.
6. Gupta, R. K.; Metzner, A. B.; Wissbrun, K. F. J Polym Eng Sci 1982, 22, 172.
7. Pearson, J. R. A.; Petrie, C. J. S. J Fluid Mech 1970, 40, 1.
8. Pearson, J. R. A.; Petrie, C. J. S. J Fluid Mech 1970, 42, 609.
9. Hyun, J. C.; Kim, H.; Lee, J. S.; Song, H.; Jung, H. W. J Non-Newtonian Fluid Mech 2004, 121, 157.
10. Han, C. D.; Park, J. Y. J Appl Polym Sci 1975, 19, 3257.
11. Macosko, C. Rheology: Principles, Measurements, and Applications; Wiley-VCH: New York, 1994.
12. Pirkle, J. C.; Braatz, R. D. Polym Eng Sci 2003, 43, 398.
13. Butler, T. I.; Patel, R.; Lai, S. Y.; Spuria, J. Proc Annu Tech Conf 1993, 52, 13.
14. Ghaneh-Fard, A.; Carreau, P. J.; Lafleur, P. G. Polym Eng Sci 1997, 37, 1148.
15. Cao, B.; Campbell, G. A. AIChE J 1990, 36, 420.
16. Gupta, R. K.; Metzner, A. B. J Rheol 1982, 26, 181.
17. Han, C. D.; Park, J. Y. J Appl Polym Sci 1975, 19, 3277.
18. Ghaneh-Fard, A.; Carreau, P. J.; Lafleur, P. G. AIChE J 1996, 42, 1388.
19. Sidiropoulos, V. Ph.D. Thesis, McMaster University, 2000.
20. Dealy, J.; Wissburn, K. Melt Rheology and Its Role in Plastics Processing; Van Nostrand Reinhold: New York, 1990.
21. Liu, C.; Bogue, D.; Spruiell, J. Int Polym Proc 1995, 10, 226.